This is an *Accepted Manuscript*, which has been through the Royal Society of Chemistry peer review process and has been accepted for publication.

Accepted Manuscripts are published online shortly after acceptance, before technical editing, formatting and proof reading. Using this free service, authors can make their results available to the community, in citable form, before we publish the edited article. We will replace this *Accepted Manuscript* with the edited and formatted *Advance Article* as soon as it is available.

You can find more information about *Accepted Manuscripts* in the **Information for Authors**.

Journal Name

ChemComm

ARTICLE TYPE

Poly β-Cyclodextrin Inclusion-induced Formation of Two-Photon Fluorescent Nanomicells for Biomedical Imaging

Huijuan Yan[a], Leiliang He[a], Cheng Ma[a], Jishan Li*[a], Jinfeng Yang[b], Ronghua Yang*[a], and Weihong Tan[a]
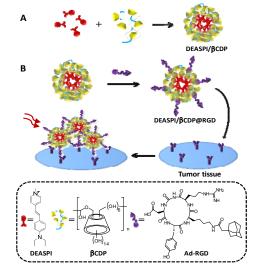
A novel two-photon absorption (TPA) nanomicell through the "host-guest" chemistry has been developed and successfully applied in tumor tissue imaging in this work.

Two-photon excitation (TPE) with near infrared (NIR) photons as the excitation source has the advantages of lower tissue auto-fluorescence and self-absorption, reduced photodamage and photobleaching, high spatial resolution and deeper penetration depth (>500 μm), etc. Together with the development of two-photon microscopy (TPM), TPE has become a powerful tool for research in life science and TP bioimaging applications.[1] The quality of two-photon fluorescence imaging in biological media is highly dependent on the two-photon absorption (TPA) materials, which should have large two-photon action cross-sections, good solubility and biocompatibility.[2] Recently, although a variety of TPA organic molecules[3] and TPA inorganic nanomaterials (e.g. metal clusters,[4] semiconductor quantum dots[5] and carbon nanomaterials[6]) have been developed and successfully applied in the fields of biomedical imaging and biosensing, the low fluorescence quantum yield and slow delivery across membranes for organic molecules, possible cytotoxicity and needition of further hydrophilic and complex functional modification process for inorganic nanomaterials, are still the limitions for their wide application in biomedical imagings. Therefore, the searching of new TPA materials with excellent characteristics such as good biocompatibility, high cell permeability and high TPA action cross-section, has become increasingly important and urgent.

Herein, as shown in Scheme 1, we constructed a β-cyclodextrin polymer (βCDP)-based TPA fluorescent nanomicell via the inclusion interaction between β-cyclodextrin (βCD) and trans-4-[p-(N,N-diethylamino) styryl]-N-methylpyridinium iodide (DEASPI) (for the synthesis of βCDP and DEASPI, see Electronic Supplementary Information (ESI)), and the further functionalized TPA fluorescent nanomicells were applied in biomedical imaging. βCD as a member of cyclodextrin (CD) family, is a widely used host molecule capable of internalizing guest molecules in water with binding constants in the $10^{0.5}$–10^5 M^{-1} range.[7] βCD and its assemblies have been extensively used for biomedical fields ranging from drug solubilization to their use as a building block for nonviral vector construction because of their high solubilization ability, low toxicity and their ability to destabilize and permeate biological membranes and for obviating undesirable side effects.[8] In our research, we found that small TPA organic molecule can be encased into the cavity of βCD to

form the βCDP-based nanomicell and the TP action cross-section of the small TPA organic molecule can be enhanced greatly. These findings have led us to exploring the design and construction of a new TPA supramolecular architecture based on the "host-guest" chemistry to apply in biomedical imaging, which has not been reported to the best of our knowledge.

Scheme 1. Schematic illustration of fabrication of the DEASPI/βCDP nanomicell (A) and application in TPE tumor tissue imaging (B).

Morphology and structure of the DEASPI/βCDP nanomicell were first investigated by using dynamic light-scattering (DLS), TEM imaging and circular dichroism spectra. DLS showed that the complex size produced by DEASPI and βCDP was about 100 nm, while the size of βCDP was only about 5.0 nm (Fig. S1, ESI). To confirm formation of the DEASPI/βCD complex via host-guest interaction, its circular dichoism spectra were measured (Fig. S2, ESI). All the solution of DEASPI, βCD and βCDP showed no significant circular dichroism spectra band, while the mixture of βCDP and DEASPI showed a strong positive Cotton band at around 470 nm, which was similar with that of the βCD/DEASPI mixture. This phenomenon can be reasoned that the achiral compounds located in the CD cavity will produce induced circular dichroism signals in the corresponding transition bands, and the sign of circular dichroism is positive for a transition polarized parallel to the axis of the macrocyclic host.[9] Both DLS and circular dichroism spectra of the samples indicate that the nanoscaled supramolecular polymer complex can be

formed under the presence of guest molecule DEASPI. Relative to the DLS results, TEM images showed that the morphology of βCDP is irregular film-shaped objects (Fig.1a) while the DEASPI/βCDP complexes exhibit the spherical geometry with the average diameters of ~ 60 nm (Fig. 1b). The sizes determined by TEM are smaller than those measured by DLS due to the relative dry nature of the TEM samples. In order to further demonstrate that the formation of nanomicell is resulted from the inducement of host-gust interaction between DEASPI and βCD rather than the encapsulation of DEASPI into the cavums of βCDP-based particles, the βCDP was first incubated with adamantine and then the DEASPI was added. DLS showed that the size of this product is about 5.0 nm similar with that of βCDP, and TEM image showed that its morphology also is irregular film shape (Fig. S3, ESI), which indicates that the DEASPI/βCDP-based nanomicells were not formed due to the formation of a more stable inclusion complexes between βCD and adamantine, demonstrating that the host-guest inclusion interaction between DEASPI and βCD is the primary factor for the formation of nanomicell.
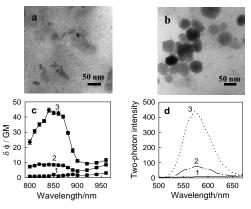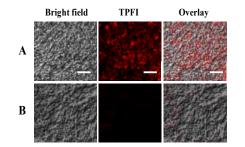

Fig. 1 TEM images of βCDP (a) and DEASPI/βCDP nanomicell (b). TPE action cross sections (c) and TPE fluorescence emission spectra (d) of the aqueous solutions. 1: 10 μM of DEASPI; 2: 10 μM of DEASPI + 0.5 mg/mL of βCD; 3: 10 μM of DEASPI + 0.5 mg/mL of βCDP. For 'c', λ_{ex} = 800-960 nm; for 'd', λ_{ex} = 840 nm.

The TPA action cross section ($\delta\Phi$, the product of the TPA cross-section (δ) and the fluorescence quantum yield (Φ)) and the TPE emission spectra of the DEASPI/βCDP nanomicell were then measured carefully. As shown in Fig. 1c, the maximal $\delta\Phi$ of DEASPI molecule in the DEASPI/βCDP nanomicell was measured to be 44.5 GM (λ_{ex} = 840 nm, 1 GM = 10^{-50} cm^4 sphoton^{-1} molecule^{-1}) with Rhodamine 6G as the reference,[10] which was much higher than that of DEASPI molecule (1.0 GM) or DEASPI/βCD inclusion complex (8.6 GM). The TPE emission spectra of the DEASPI/βCDP nanomicell are shown in Fig. 1d. One can see that the TPE fluorescence emission intensity of this nanomicell can be enhanced up to ca 40 times compared to that when DEASPI is directly dissolved in aqueous solution, while only about 5-times enhancement is observed when βCD monomer was used. These TPE fluorescence emission spectra are similar with those by one-photon excitation (OPE) experiments (Fig. S4, ESI), very weak one photon-induced emission was also observed for either DEASPI or DEASPI/βCD owing to their lower fluorescence quantum yield (The Φ is 0.47, 0.02 and 0.10 for DEASPI/βCDP, DEASPI or DEASPI/βCD inclusion complex,

respectively (Table S1, ESI)), indicating that the formation of nanomicell can offer a more protective microenvironment to decrease the effect of twisted intra-molecular charge transfer (TICT) process on the embedded DEASPI.

Stability of the prepared nanomicell under various environmental conditions, for example different pH value, different ions's concentrations (Na$^+$, K$^+$, Ca^{2+}, Mg^{2+}), human serum or human cell lysate-contained biological fluids and irradiation by using a 150 W xenon lamp as the excitation source, was first investigated through testing its fluorescence intensity Fig. S5, ESI). The results show that the prepared fluorescent nanomicell has good photostability and is stable under around physiological pH value, high ion strength, biological condition and a long storage time. Furthermore, cellular cytotoxicity assay of the DEASPI/βCDP nanomicell towards HeLa and MCF-7 cells as the model shows that no apparent cytotoxicity was observed to these two cells even when the concentration of this nanomicell was increased up to 2.5 mg/mL (~ 50 μM DEASPI) (Fig. S6, ESI). The cytotoxicity of this nanomicell is much lower than that of the DEASPI molecules alone which killed 32% HeLa cells and 22% MCF-7 cells respectively at the similar amount of materials. The high biocompatibility of βCDP and the efficient shielding of organic molecules by the matrix in βCDP-based nanomicell may be a cause of the low cytotoxicity of this TPA nanomicell to cells.
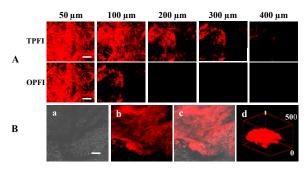

Fig. 2 TPE fluorescence images of frozen cervical cancer tumor tissue slice (A) and frozen normal cervical tissue slice (B) stained by DEASPI/βCDP@RGD. Scale bars: 40 μm.

To demonstrate the practical applications of this prepared TPA nanomicell in biomedical imaging or clinical diagnostics, a cyclic RGD peptide (c(RGDyK)) conjugated adamantine (denoted as Ad-RGD) was anchored on the surface of the βCDP-based nanomicell to form TPA bionanoprobe (DEASPI/βCDP@RGD) by the βCD/Adamantine host-guest inclusion strategy (Scheme 1B, Fig. S7 in ESI). The c(RGDyK) selectively recognizes $\alpha_v\beta_3$ and $\alpha_v\beta_5$ integrin receptors, which plays a pivotal role in angiogenesis, vascular intima thickening, and proliferation of malignant tumors.[11] HeLa cells possessing $\alpha_v\beta_3/\alpha_v\beta_5$ integrins and integrin-negative cells (MCF-7) were first chosen as model cell lines to investigate the targeting effect.[12] It can be seen clearly from Fig. S8 (ESI) that DEASPI/βCDP@RGD did not bind to integrin-negative cells (MCF-7) after a 30 min-incubation time because there is minimal fluorescence signal observed, whereas the integrin-positive cells (HeLa) are clearly visualized and the staining can be blocked effectively by 10 μM c(RGDyK). Additionally, non-RGD-conjugated DEASPI/βCDP nanomicell had minimal nonspecific binding under the same incubation time of 30 min. These results demonstrate that the DEASPI/βCDP@RGD can selectively bind to integrin $\alpha_v\beta_3/\alpha_v\beta_5$-

riched tumor cells. Next the DEASPI/βCDP@RGD were used for imaging diagnosis of cervical cancer. Fig. 2 shows the DEASPI/βCDP@RGD staining of frozen slices of the cervical tumor tissues and the normal cervical tissues, respectively. Strong fluorescence signals can be observed for the cervical tumor tissue slice, while the normal cervical tissue slice gave virtually no fluorescence signal. Moreover, no obvious fluorescence was noted for both the cervical tumor tissue slice and the normal cervical tissue slice stained with DEASPI/βCDP (Fig. S9, ESI). The above confocal images clearly demonstrate the high $\alpha_v\beta_3/\alpha_v\beta_5$ integrins expression level of the cervical cancer.

Fig. 3 Confocal fluorescence images of a part of a fresh thick cervical tumor tissue slice stained by DEASPI/βCDP@RGD. (A) Z-scan TPE (TPFI) and OPE (OPFI) fluorescence images at different penetration depths, the scale bar is 80 μm; (B) Bright-field image (a), TPE fluorescence image (b), overlay image (c) and the 3D reconstruction from 50 Z-scan TPE imaging sections at depth of 0–500 μm with 60×magnification (d), the scale bar is 60 μm.

To further demonstrate the deep imaging capacity of the prepared TPA nanomicell, after incubation of a 2.0 mm-thick cervical tumor tissue slice with the DEASPI/βCDP@RGD, the fluorescence imagings were performed by two-photon confocal microscopy. The Z-scanning confocal imaging shows that bright TPE fluorescence emission was still present until the 300 μm of penetration depth, while no significant OPE fluorescence can be observed when the penetration depth was only more than 100 μm (Fig. 3A), indicating that the prepared TPA nanomicell has the capacity of depth tissue imaging. Then the 3D reconstitution of confocal XYZ scanning micrographs is obtained from 50 confocal Z-scan TPE imaging sections ('d' of Fig. 3B), which indicates the DEASPI/βCDP@RGD nanoprobes are evenly distributed in HeLa tissues and have a high signal-to-noise ratio.

In conclusion, a facile strategy for TPA fluorescent nanomicell preparation has been developed through the "host-guest" chemistry. This βCDP-based TPA fluorescent nanomicell exhibits desirable two-photon-sensitized fluorescence properties, high photostability, high cell-permeability, high stability and excellent biocompatibility. As a result, by anchoring the RGD peptide on the nanomicells's surface via the high binding affinity of labeled adamantine with βCD, the targeted TPE imaging has been successfully achieved in cancer cells and tumor tissues. To the best of our knowledge, it is the first time that βCDP-based two-photon fluorescent nanoprobe has been successfully used in cancer cells and tissues. The material design approach reported here also open up new perspectives for developing a wide range of unique sensing schemes and will have great potential in cancer diagnosis and biomedical research, which are compatible with the benefits of multiphoton imaging techniques.

Notes and references

a State Key Laboratory of Chemo/Biosensing and Chemometrics, College of Chemistry and Chemical Engineering, Hunan University, Changsha 410082, China. Tex/Fax: +86 731 88822587. E-mail: jishanli@hnu.edu.cn, yangrh@pku.edu.cn
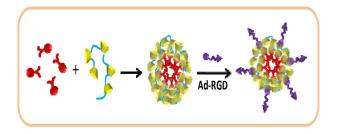*b Tumor Hospital of Xiangya School of Medicine, Central South University, Changsha 410013, China.*
†Electronic Supplementary Information (ESI) available: Experimental details, synthesis and characterization of DEASPI and βCDP, one-photon luminescence spectra and the photostability test, MTT assay and targeted cell two-photon imaging. See DOI: 10.1039/c000000x/

1 (a) F. Helmchen and W. Denk, *Nat. Method.* 2005, **2**, 932-940; (b) D. A. Parthenopoulos and P. M. Rentzepis, *Science.* 1989, **245**, 843-845; (c) S. Kawata and Y. Kawata, *Chem. Rev.* 2000, **100**, 1777-1788; (d) H. M. Kim and B. R. Cho, *Acc. Chem. Res.* 2009, **42**, 863-872; (e) H. J. Kim, C. H. Heo, and H. M. Kim, *J. Am. Chem. Soc.* 2013, **135**, 17969−17977; (f) S. K. Bae, C. H. Heo, D. J. Choi, D. Sen, E.-H. Joe, B. R. Cho, and H. M. Kim, *J. Am. Chem. Soc.* 2013, **135**, 9915−9923.
2 (a) S. Kim, Q. D. Zheng, G. S. He, D. J. Bharali, H. E. Pudavar, A. Baev and P. N. Prasad, *Adv. Funct. Mater.* 2006, **16**, 2317-2323; (b) K. Li, Y. H. Jiang, D. Ding, X. H. Zhang, Y. T. Liu, J. L. Hua, S. S. Feng and B. Liu, *Chem. Commun.* 2011, **47**, 7323-7325.
3 (a) G. S. He, L. S. Tan, Q. D. Zheng and P. N. Prasad, *Chem. Rev.* 2008, **108**, 1245-1330; (b) S. Sumalekshmy and C. J. Fahrni, *Chem. Mater.* 2011, **23**, 483-500; (c) S. Yao and K. D. Belfield, *Eur. J. Org. Chem.* 2012, **17**, 3199-3217.
4 (a) G. Ramakrishna, O. Varnavski, J. Kim, D. Lee and T. Goodson, *J. Am. Chem. Soc.* 2008, **130**, 5032-5033; (b) S. A. Patel, C. I. Richards, J. C. Hsiang and R. M. Dickson, *J. Am. Chem. Soc.* 2008, **130**, 11602-11063.
5 (a) J. Z. Wang, M. Lin, Y. L. Yan, Z. Wang, P. C. Ho and K. P. Loh, *J. Am. Chem. Soc.* 2009, **131**, 11300-11301; (b) L. Jauffred and L. B. Oddershede, *Nano Lett.* 2010, **10**, 1927-1930; (c) E. J. McLaurin, A. B. Greytak, M. G. Bawendi and D. G. Nocera, *J. Am. Chem. Soc.* 2009, **131**, 12994-13001.
6 (a) J. L. Li, H. C. Bao, X. L. Hou, L. Sun, X. G. Wang and M. Gu, *Angew. Chem. Int. Ed.* 2012, **51**, 1830-1834; (b) B. Kong, A. W. Zhu, C. Q. Ding, X. M. Zhao, B. Li and Y. Tian, *Adv. Mater.* 2012, **24**, 5844-5848; (c) A. W. Zhu, Q. Qu, X. L. Shao, B. Kong and Y. Tian, *Angew. Chem. Int. Ed.* 2012, **51**, 7185-7189.
7 M. V. Ekharsky and Y. Inoue, *Chem. Rev.* 1998, **98**, 1875-1918.
8 (a) A. Harada, *Acc. Chem. Res.* 2001, **34**, 456-464; (b) A. Kulkarni, K. DeFrees, S. Hyun and D. H. Thompson, *J. Am. Chem. Soc.* 2012, **134**, 7596-7599; (c) J. X. Zhang, H. L. Sun and P. X. Ma, *Acs Nano.* 2010, **4**, 1049-1059.
9 B. Balan, D. L. Sivadas and K. R. Gopidas, *Org. Lett.* 2007, **9**, 2709-2712.
10 N. S. Makarov, M. Drobizhev and A. Rebane, *Opt. Express.* 2008, **16**, 4029-4047.
11 (a) F. Danhier, A. L. Breton and V. Préat, *Mol. Pharmaceutics.* 2012, **9**, 2961-2973; (b) M. Théry, V. Racine, A. Pepin, M. Piel, Y. Chen, J. B. Sibarita and M. Bornens, *Nat. Cell Biol.* 2005, **7**, 947-953.
12 (a) M. Oba, K. Aoyagi, K. Miyata, Y. Matsumoto, K. Itaka, N. Nishiyama,Y.Yamasaki, H. Koyama and K. Kataoka, *Mol. Pharmaceutics.* 2008, **5**, 1080-1092; (b) M. Oba, S. Fukushima, N. Kanayama, K. Aoyagi, N. Nishiyama, H. Koyama and K. Kataoka, *Bioconjugate Chem.* 2007, **18**, 1415-1423.

TOG:

The obtained nanomicell through "host-guest" chemistry exhibits desirable TPA property and can further conjugate with functional receptors.